

Published in final edited form as:

J Immunol. 2012 November 1; 189(9): 4621–4629. doi:10.4049/jimmunol.1200828.

Coordinate Stimulation of Macrophages by Microparticles and TLR Ligands Induces Foam Cell Formation¹

Peter A Keyel^{*,2}, Olga A. Tkacheva[†], Adriana T. Larregina^{*,†}, and Russell D Salter^{*,2}

^{*}Department of Immunology, University of Pittsburgh, Pittsburgh, PA 15260

[†]Department of Dermatology, University of Pittsburgh, Pittsburgh, PA 15260

Abstract

Aberrant activation of macrophages in arterial walls by oxidized lipoproteins can lead to atherosclerosis. Oxidized lipoproteins convert macrophages to foam cells through lipid uptake and TLR signaling. To investigate the relative contributions of lipid uptake and TLR signaling in foam cell formation, we established an in vitro assay utilizing liposomes of defined lipid compositions. We found that TLRs signaling through Trif promoted foam cell formation by inducing both NF- κ B signaling and Type I IFN production, whereas TLRs that do not induce IFN, like TLR2, did not enhance foam cell formation. Addition of IFN α to TLR2 activator promoted robust foam cell formation. TLR signaling further required PPAR α , as inhibition of PPAR α blocked foam cell formation. We then investigated the ability of endogenous microparticles (MP) to contribute to foam cell formation. We found that lipid containing MP promoted foam cell formation, which was enhanced by TLR stimulation or IFN α . These MP also stimulated foam cell formation in a human skin model. However, these MP suppressed TNF α production and T cell activation, showing that foam cell formation can occur by immunosuppressive microparticles. Taken together, the data reveal novel signaling requirements for foam cell formation and suggest that uptake of distinct types of MP in the context of activation of multiple distinct TLR can induce foam cell formation.

Keywords

microvesicle; foam cell; streptolysin; ectosome

Introduction

Macrophages are one of the first line responders of the innate immune system. As such, they help coordinate the immune response to pathogens and other forms of danger. Correct signaling is vital to a protective immune response, and aberrant activation can lead to a number of diseases, including atherosclerosis (1). Indeed, a prominent characteristic of atherosclerosis, the formation of fatty streaks, is caused by conversion of macrophages into foam cells. Foam cell formation is characterized by an accumulation of lipids, predominantly cholesterol esters (1, 2). Oxidized LDL (oxLDL) is the archetypal source of cholesterol and inducer of foam cell formation (1). However, other lipids can also contribute to foam cell formation. For example, treatment of macrophages with LPS and LDL can lead to foam cell formation, even without oxidation of LDL (3).

¹This work was supported by NIH grants AI072083 and CA073743. PAK was supported by training grant T32CA82084.

²to whom correspondence should be addressed: Russell Salter, E1052 BST, 200 Lothrop St, Pittsburgh, PA 15260, tel: (412) 648-9471, fax: (412) 383-8096, rds@pitt.edu. Peter Keyel, E1053 BST, 200 Lothrop St, Pittsburgh, PA 15260, tel: (412) 648-8468, fax: (412) 383-8096, pak55@pitt.edu.

LPS signals through Toll-like receptor (TLR) 4. TLRs are sensors of pathogen-associated molecular patterns, including molecules which range from bacterial and viral nucleic acids to bacterial and fungal cell wall components. Typically TLRs signal through adaptors, the best understood being Trif and MyD88, which propagate the immune response through activation of NF- κ B, AP-1 and/or Type I IFN production (4). TLR signaling in the context of pathogen infection can lead to atherosclerosis. For example, activation of TLR2 by Chlamydia leads to enhanced atherosclerosis (5). OxLDL itself can signal through a CD36/TLR4/TLR6 heterotrimer to induce foam cell formation (6), though it has also been reported that oxLDL impairs LPS-induced NF- κ B signaling (7, 8). One way in which TLR4 controls foam cell formation is through induction of cellular programs that alter the metabolic state of a macrophage (9). These changes are designed to trap and eliminate internalized pathogens, but they also result in decreased cholesterol efflux, which enhances foam cell formation (10). Thus, TLR4 can influence foam cell formation, though the signaling requirements remain unclear.

OxLDL and LDL are not the only lipid sources that can promote foam cell formation. Exosomes derived from T cells have also been implicated in foam cell formation (11). Unlike oxLDL, these exosomes are internalized by the phosphatidylserine receptor on macrophages (11). Microparticles (MP) derived from endothelial cells and platelets have also been implicated in a number of cardiovascular diseases, including hypertension, coronary and peripheral artery diseases, and atherosclerosis (12). Indeed, MP are increased in patients with cardiovascular disease (12) and can be predictive of disease (13). MP also lead to neovascularization, progression and eventual destabilization of atherosclerotic plaques (14). MP can promote vascular inflammation and expression of inflammatory cytokines, partially through delivery of IL-1 β to endothelial cells (15). They can also lead to macrophage apoptosis (16). Many of these functions have been attributed to the protein profile of the MP (12). However, what role the lipids present in the MP play is less well understood. Similarly, the role of MP in the initial stage of foam cell formation is poorly understood.

We hypothesized that foam cell formation requires both activation through a TLR pathway and any source of abundant exogenous lipid. OxLDL fulfills both of these requirements, and can drive foam cell formation independently of other ligands. In the present study, we further investigated additional TLR ligands and biologically relevant lipid sources, specifically non-oxidized MP, that might also promote foam cell formation.

Materials and Methods

Reagents

Unless otherwise noted, reagents were from Sigma-Aldrich (St Louis, MO). Phosphatidylcholine, phosphatidylserine and phosphatidylethanolamine were from Avanti Polar Lipids (Alabaster, AL). Ultrapure LPS, N-palmitoyl-S-[2,3-bis(palmitoyloxy)-(2RS)-propyl]-[R]-cysteinyl-[S]-seryl-[S]-lysyl-[S]-lysyl-[S]-lysyl-[S]-lysine (Pam3CSK4), polyinosine-polycytidilic acid (polyI:C) and Type B CpG-ODN were purchased from Invivogen (San Diego, CA). Anti-CD69 conjugated to FITC and anti-CD80 conjugated to APC antibodies were from BD Biosciences (San Jose, CA). Streptolysin O (SLO) was purified from *E. coli* as previously described (17). LDL and oxLDL were from Biomedical Technologies (Stoughton, MA).

Cell culture

BMDM were isolated and cultured as previously described (18). Bone marrow from B6, TLR4^{-/-}, MyD88^{-/-}, and Trif^{-/-} mice were generous gifts from Lisa Borghesi and Timothy

Billiar. HeLa, D2, TA3/Ha and B16 cells were cultured in DMEM supplemented with 10% FCS, 2 mM L-glutamine, 100 U/mL penicillin and 100 U/mL streptomycin. 3T3 cells were also cultured in this medium, though it was fortified with 1 mM sodium pyruvate and 1x non-essential amino acids. To rule out microparticle contamination from FCS, TA3/Ha cells were also cultured in AIM V media (Invitrogen, Carlsbad, CA). T27A cells were cultured in RPMI supplemented with 10% FCS, 2 mM L-glutamine, 100 U/mL penicillin and 100 U/mL streptomycin. B3Z cells were also cultured in this media, along with 500 μ g/mL G418. Human macrophages were differentiated from plastic-adhered PBMCs obtained anonymously from the Central Blood Bank (Pittsburgh, PA) in DMEM supplemented with 10% FCS, 2 mM L-glutamine, 100 U/mL penicillin and 100 U/mL streptomycin and 10 ng/mL GM-CSF for 5 days.

Liposome preparation

Liposomes were prepared as previously described (19). Individual lipids in chloroform or ethanol (cholesterol) were mixed at a molar ratio of 45:45:10:0 or 22.5:22.5:10:50 phosphatidylcholine:phosphatidylethanolamine:phosphatidylserine:cholesterol (Ochol and 50chol liposomes, respectively) in glass tubes and dried under nitrogen. The lipids were resuspended in 15 mM HEPES, pH 7.4, 50 mM sorbitol, 1 mM magnesium acetate at a concentration of 4 mg/mL and incubated at 37°C for 1 hr. Liposomes were formed through 4 freeze-thaw cycles and stored -80°C. No oxidation of the liposomes was detected by TBARS assay nor was LPS detected by LAL assay.

Microparticle preparation

Spontaneously released vesicles (SRV) were prepared by collecting the supernatant of cells cultured for 2–3 days at 37°C and centrifuging first at 300xg and then at 107,000xg using a Sorvall Surespin 630/36 rotor. The pellet was resuspended in RPMI and used for assays. For ectosome (MV) production, 50–100 million target cells were harvested, centrifuged at 300xg and resuspended in RPMI. SLO was added at a sublytic dose (300–1500 U/mL, depending on cell type) and the cells incubated at 37°C for 15 min. The cells were pelleted at 300xg and the MV isolated from the supernatant via centrifugation at 107,000xg using a Beckman SW60 Ti rotor. The pellet was resuspended in RPMI. Protein content was determined by Bradford assay, and cholesterol content colorimetrically according to manufacturer instructions (Cayman Chemicals, Ann Arbor, MI). EM analysis was performed by adsorbing MP onto EM grids for 10 min at room temperature, and staining for 30 seconds with 1% uranyl acetate. Grids were examined on a JEOL 1011 transmission EM.

Foam cell assay

10⁵ BMDM were incubated in IMDM supplemented with 10% FCS, 1x L-glutamine and 100 U/mL penicillin and 100 U/mL streptomycin for 2 days in the presence or absence of 112 μ g/mL liposomes, 25 μ g/mL MV or SRV, 1 μ g/mL Pam3CSK4, 10 ng/mL LPS, 10 μ g/mL polyI:C, 1.68 μ M CpG, 100 U/mL IFN α (PBL Interferon Source, Piscataway, NJ), and fixed in 2% p-formaldehyde for 15 min. Cells were washed in 60% isopropanol, stained with 0.3% oil red O in 60% isopropanol, washed once each in 60% isopropanol and PBS, stained for 1 min with Harris Hematoxylin, washed in PBS, blued with Scott's water for 1 min, washed in PBS and mounted in gelvatol. Images were acquired on an Olympus Provis using a 40x objective. All macrophages containing one or more Oil Red O positive lipid droplets were counted as foam cells, consistent with previous methods (20). Foam cell formation was also assessed by measuring the intensity of Oil Red O staining using Metamorph. Images were separated into red/green/blue images and the green image subtracted from the red to provide the Oil Red O specific image. An image mask was prepared through dilation and erosion, and the integrated intensity above background was measured. This intensity was normalized to the number of cells in the field. The per cell

intensity was expressed as a percentage of the maximal intensity in the experimental set which enabled comparison across sets. Filtration of the media through a 0.1 μm filter to remove serum MP did not alter the extent foam cell formation (data not shown).

Cholesterol Assay

5×10^5 BMDM were incubated in IMDM supplemented with 10% FCS, 1x L-glutamine and 100 U/mL penicillin and 100 U/mL streptomycin for 2 days in the presence or absence of 112 $\mu\text{g}/\text{mL}$ liposomes, 10 ng/mL LPS or 10 $\mu\text{g}/\text{mL}$ polyI:C, fixed in 2% p-formaldehyde for 15 min and washed in PBS and 60% isopropanol. Cholesterol was extracted with 250 μL isopropanol for 30 min at room temperature, and cholesteryl esters measured using a fluorimetric cholesterol assay (Cayman Chemicals) according to manufacturer's instructions. Protein was extracted using 0.1 M NaOH and measured by Bradford Assay.

Skin assays

Samples of normal human skin were obtained from healthy donors undergoing abdominal plastic surgery and distributed by the tissue bank, a division of the Department of Pathology of the University of Pittsburgh Medical Center. Human skin samples obtained following de-identification by honest brokers are classified as human non-subjects by our IRB. Skin explants composed by epidermis and dermis were obtained by a dermatome as previously published (21) and injected with either oxLDL, 50chol liposomes or MV. Following 3 days, skin samples were paraffin embedded, sectioned and stained with hematoxylin and eosin and analyzed by light microscopy using an Axiostar plus microscope (Zeiss).

Activation status of BMDM

5×10^5 BMDM were incubated with lipids and/or TLR ligands for 18 h at 37°C, harvested with Cellstripper (Cellgro, Mannassas, VA) stained with antibodies for 30 min on ice and analyzed by FACS using an LSR II. Supernatants were saved for measurement of TNF α by ELISA (BioLegend, San Diego, CA)

B3Z Assay

T cell activation was measured as previously described (22). Briefly, 10^4 B3Z cells were cultured at 37°C overnight in 96-well plates in the presence or absence of 0.1–100 ng/mL OVA peptide (SIINFEKL), 5000 B16 cells, 112 $\mu\text{g}/\text{mL}$ liposomes or 25 $\mu\text{g}/\text{mL}$ MV. B3Z cells were washed, incubated for 4 hr at 37°C in 150 μM chlorophenol red- β -D-galactopyranoside (CPRG) and 0.1% Triton X-100 and A₅₇₅ read on a PowerWave XS plate reader (BioTek, Winooski, VT).

Statistics

Statistics were determined with Two-way ANOVA followed by Bonferroni post-testing using Prism3.0 (GraphPad, La Jolla, CA).

Results

Multiple types of lipid MP induce foam cell formation

To dissect the relationship between TLR signaling, lipids and foam cell formation, we compared the ability of oxLDL, LDL and liposomes with defined compositions to promote foam cell formation in bone-marrow derived macrophages (BMDM) with or without LPS by Oil Red O staining. Although LPS alone did not promote any foam cell formation, oxLDL robustly did so regardless of LPS, consistent both with its own ability to activate TLR4 and ability to antagonize LPS-induced signaling (6–8) (Fig 1A, B). As previously reported (3), LDL promoted foam cell formation in the presence of LPS (Fig 1C). We tested the ability of

liposomes either lacking cholesterol (0chol) or comprised of 50% cholesterol (50chol) to promote foam cell formation. We found that in the absence of cholesterol, liposomes only stimulated foam cell formation in the presence of LPS (Fig 1D). Consistent with the ability of cholesterol to drive foam cell formation (1), 50chol liposomes promoted foam cell formation without LPS, though LPS further enhanced this effect (Fig 1E). Thus, LPS can enhance or even drive foam cell formation in the presence of exogenous lipids.

TLR4 independent foam cell formation

Since LPS enhanced foam cell formation, we asked if the spontaneous formation of foam cells in the presence of cholesterol containing liposomes was due to TLR4 activation. We determined that the liposome preparations were endotoxin-free by LAL assay, and then tested whether they stimulated foam cell formation in TLR4^{-/-} macrophages singly, or in combination with either LPS, or the TLR3 ligand polyI:C. Both TLR ligands promoted robust foam cell formation in B6 BMDM (Fig 1F). We found that TLR4^{-/-} BMDM were able to form foam cells following liposome treatment (Fig 1G) when co-exposed to polyI:C, but not to LPS (Fig 1G). Quantitation of the Oil Red O staining in these macrophages showed that an increase in the amount of cholesterol in the liposomes increased the severity of foam cell formation (Supplemental Figure S1A, B). Oil Red O staining recapitulated cholesteryl ester levels, as LPS and polyI:C both induced an increase in cholesteryl esters (Supplemental Fig S1C). We next asked if 0chol or 50chol liposomes could induce foam cell formation in primary human macrophages. The human macrophages had a higher degree of spontaneous foam cell formation in culture (Supplemental Fig S1D), which has been observed in other systems (23). The 50chol liposomes significantly increased this basal level of foam cell formation (Supplemental Fig S1D) in the presence or absence of LPS. Taken all together, these data show that TLR3, in addition to TLR4, can promote foam cell formation.

Synergism between TLR and type I IFN signaling for foam cell formation

To determine if multiple TLRs could promote foam cell formation, we treated macrophages with either 0chol or 50chol liposomes and ligands for TLR2, 3, and 4. While we found that stimulation through TLR3 and TLR4 increased the incidence of foam cell formation with either 0chol and 50chol liposomes as a lipid source (Fig 2A), TLR2 did not provide significant augmentation when ligated with Pam3CSK4. Since TLR2 activation by Pam3CSK4 is mediated at the cell surface, we considered whether TLRs that function in endosomes might selectively enhance foam cell formation. Traditionally, TLRs are divided into surface TLRs, that predominantly signal at the surface, and endosomal TLRs that predominantly signal following internalization. The surface TLRs signal predominantly through MyD88, leading only to NF-KB activation. The endosomal TLRs signal through Trif (TLR3 and TLR4) or MyD88 (TLR4, TLR9), leading to both NF-KB and IRF3 (Trif) or IRF7 (MyD88) activation (4). IRF signaling leads to Type I IFN production (4). To test whether Type I IFN production is responsible for the observed difference in the ability of surface and endosomal TLRs to enhance foam cell formation, we added IFN α in combination with liposomes to BMDM. IFN α promoted foam cell formation only in 50chol liposomes, but not 0chol liposomes (Fig 2B). Since the other primary signaling outcome of TLR signaling is NF-KB activation, we asked if treatment with both IFN α and Pam3CSK4, neither of which independently promote 0chol liposome-mediated foam cell formation, would enhance foam cell formation. We found that the combination of Pam3CSK4 and IFN α together with either 0chol or 50chol liposomes drove robust foam cell formation, measured either by total number of foam cells or intensity of Oil Red O staining (Fig 2). This was comparable to the foam cell formation provided by LPS or polyI:C and liposomes (Fig 2). Thus, Type I IFN enhances foam cell formation.

Trif is required for polyI:C and LPS dependent foam cell formation

To further probe the signaling role TLRs play in foam cell formation, we asked which TLR adaptors were responsible for foam cell formation. We treated BMDM from wild type, Trif^{-/-}, or MyD88^{-/-} mice with no lipid, 0chol or 50chol liposomes and various TLR ligands. Ablation of Trif reduced the spontaneous foam cell formation that occurs following polyI:C treatment (Fig 3A). Foam cell formation due to 0chol liposomes in the presence of polyI:C was Trif dependent (Fig 3B). Foam cell formation following treatment with 50chol liposomes was Trif dependent, as was the enhancement of foam cell formation by either LPS or polyI:C (Fig 3C). No significant difference was observed between wild type and knockout mice when treated with Pam3CSK4+IFN α (Fig 3B, C), indicating TLR adaptor deficiencies could be overcome. Thus, we believe that both Type I IFN and NF- κ B signaling, which are provided by TLR ligation, may be needed for liposome-mediated foam cell formation.

Activation of PPAR α but not PPAR γ enhances foam cell formation

TLR ligation has previously been implicated in atherogenic signaling factors. For example, in a transfected cell system, IRF3 can act as a switch between LXR activation and foam cell formation in an IFN-independent manner (24). Given that LXR activation can also lead to PPAR γ activation, which is anti-atherogenic (25), we wanted to determine what role PPAR played in microparticle induced foam cell formation. When we treated macrophages with agonists or antagonists to PPAR γ in the presence of TLR ligands and liposomes, we found no effect on the extent of foam cell formation (data not shown). Similarly, the LXR agonist GW3965 had no effect on foam cell formation in our system (data not shown). However, we found that PPAR α agonists and antagonists had a profound effect on foam cell formation. Fenofibrate, a PPAR α agonist, promoted foam cell formation in macrophages treated with either 0chol or 50chol liposomes (Fig 4A). Conversely, GW6471, a PPAR α antagonist, blocked foam cell formation by 50chol liposomes (Fig 4A). Although GW6471 did not significantly change the number of foam cells formed by treatment with LPS and 0chol, it did reduce the overall Oil Red O staining (Fig 4). When BMDM were treated with LPS and liposomes, fenofibrate further augmented foam cell formation by 0chol liposomes (Fig 4B). Conversely, GW6471 impaired foam cell formation by the combination of either 0chol or 50chol liposomes and LPS (Fig 4B). Thus, PPAR α activation plays a decisive role in foam cell formation.

Foam cell formation by endogenous lipid bearing vesicles

To further characterize the requirements for lipid sources that could promote foam cell formation and substantiate the biological relevance of these findings, we next addressed whether endogenous MP could promote foam cell formation. T cell derived exosomes promote foam cell formation (11). MP similarly play a role in atherogenesis (26). We examined the ability of two types of MP to promote foam cell formation, and whether the TLR pathway operative with liposomes was used. One source of MP was spontaneously released vesicles (SRV) by TA3/Ha adenocarcinoma or B16 melanoma cells. Electron microscopic examination of SRV derived from TA3/Ha or B16 cells indicated that they were 80–100 nm in size, consistent with exosomes (Supplemental Fig S2A, B). A second source of MP was microvesicles shed by cells in response to damage by toxins (MV), also known as ectosomes (17, 27–29). Ectosomes are shed as part of the cellular resistance mechanism to pore-forming toxins (17, 30), and may be taken up by macrophages responding to the bacterial infection. MV prepared from four different cell lines were larger and more heterogeneous than SRVs (Supplemental Fig S2C-F), as previously described (30). As expected from membranes containing large numbers of cholesterol-binding toxin pores, MV were significantly enriched in cholesterol relative to their parent cell line (Supplemental Fig S2G). We compared the ability of SRV and MV to promote foam cell

formation with oxLDL. Both SRV and MV stimulated varying degrees of foam cell formation (Fig 5A, and Supplemental Fig S3). We found that cholesterol content of the MV correlated with robustness of foam cell formation, reminiscent of 0chol and 50chol liposomes (Fig 5A and Supplemental Fig S2G). Thus, two types of MP, SRV and MV, both promote foam cell formation, and this is correlated with the amount of cholesterol present in the shed vesicle.

We next determined what role TLR and PPAR signaling played in enhancing microparticle-driven foam cell formation. Unlike oxLDL or SRV, LPS enhanced the formation of foam cells stimulated by MV (Fig 5A). Even MV that contained relatively low amounts of cholesterol showed enhanced foam cell formation when treated with LPS (Fig 5A). Treatment with either polyI:C or both Pam3CSK4 and IFN α also enhanced SRV and MV-induced foam cell formation (data not shown). Treatment with PPAR agonists and antagonists similarly promoted or reduced expression as observed with the liposomes (Fig 5B). Finally, given that macrophages can signal through p38 in response to ATP-derived MP (31), we tested whether p38 played a role in foam cell formation. We found that chemical inhibition of p38 with SB203580 had no effect upon foam cell formation (Fig 5A). Thus, MV show similar TLR and PPAR dependence for foam cell formation as liposomes.

MP Promote Foam Cell Formation in Tissue

We next asked whether MP were capable of inducing foam cell formation in a tissue model. We utilized total human skin because it was a readily available source of healthy tissue for which the histology is well understood and manipulations easily performed (21). Vessel triads present in the skin contain endogenous macrophages, removing the variable of cell migration into the tissue. Importantly, injection of PBS intradermally led only to limited edema three days later, and no disruption of vessel triads (Fig 6A). Injection of oxLDL, however, led to lipid accumulation in macrophages, and a classic foam cell phenotype (Fig 6B, thick arrowheads). Similarly, injection of MV derived from B16 or 3T3 cells led to foam cell formation, as did injection of SRV and 50chol liposomes (Fig 6C–F, thick arrowheads). The melanin present within B16 MP allowed us to confirm that these MP were internalized by the foam cells (Fig 6C, E, thin arrowheads). To confirm that the foam cells were macrophages, frozen sections of oxLDL-treated tissue were cut and dual stained with the macrophage marker anti-CD68 and endothelial marker anti-CD31 (Fig 6G, H). Although CD31+ cells did not show any foam cell formation, CD68+ cells in the vessel triad did become foamy, as seen by dilution of the CD68 signal and lipid inclusions present in the cell (compare intensity of CD68 staining in Fig 6G and Fig 6H). Thus, we conclude that MP can promote foam cell formation in tissue.

Endogenously derived MP only weakly activate macrophages in the absence of TLR ligands

One difference between foam cell formation due to MP and that due to oxLDL is the need of MP for an exogenous TLR ligand. To determine whether there are other differences in macrophage phenotype, we tested the ability of MP or oxLDL to activate macrophages after 18 hours. We found that LPS induced surface CD69 expression on a large percentage of cells, and CD80 to a lesser extent (Fig 7). Similarly, oxLDL induced primarily CD69, but also CD80 (Fig 7). In contrast, MV induced CD80 expression and minimal CD69 induction (Fig 7). Both 0chol and 50chol liposomes did not induce either CD69 or CD80 surface expression (data not shown). Thus, we observe distinct effects of oxLDL and MP on macrophages, even though both sources can drive macrophages to become foam cells.

SRV and MV suppress T cell function

Since we observed limited activation of BMDM treated with MV or SRV, we measured the ability of BMDM to produce TNF α following TLR stimulation. When BMDM were treated with either LPS or TLR9 ligand CpG, they produced large amounts of TNF α (Fig 8A). In the presence of MV or SRV, the TNF α production was attenuated (Fig 8A). SRV were not as able to impair TNF α production as robustly as MV (Fig 8A).

To confirm that MP were acting in an immunosuppressive manner, we tested their ability to block antigen stimulation of the B3Z T cell hybridoma. B3Z cells secrete β -galactosidase in response to stimulation through H2-K^b with the ovalbumin peptide SIINFE(H/K)L (OVA peptide) (22). We incubated B3Z cells with OVA peptide, B16 cells (which express H2-K^b), and B16 or 3T3-derived MV or SRV and measured β -galactosidase activity. We found that both MV and SRV blocked activation following treatment with 0.1 nM OVA peptide, though this inhibition could be overcome with a 100-fold increase in OVA peptide (Fig 8B). B3Z cells can also present OVA peptide to one another, although the efficiency is greatly reduced (Fig 8C). MV and SRV also blocked this activation of B3Z cells (Fig 8C). These data indicate that MV and SRV are immunosuppressive, and yet can promote foam cell formation.

Discussion

Here we have dissected the novel signaling pathways leading to foam cell formation. We have characterized a pathway for foam cell formation wherein three signals are required: exogenous lipid, NF-KB signaling and IFN α . These signals lead to PPAR α activation and subsequent foam cell formation. We offer support for the hypothesis that in the presence of TLR ligands, MP, such as ectosomes or SRV, promote foam cell formation, even though these MP are themselves weakly activating or inhibitory.

These data shed light on the link between TLR activation and foam cell formation. We find here that both NF-KB and Type I IFN production are required for optimal foam cell formation. OxLDL activates both arms of this pathway through its interaction with TLR4. TLR ligands that do not accomplish both of these functions, such as TLR2, are predicted to require another source of Type I IFN for optimal foam cell formation. In Chlamydia infection, TLR2 is critically required for foam cell formation (5). Stimulation with zymosan, a potent TLR2 ligand, however, did not result in foam cell formation (32). The model presented here resolves this seeming paradox, as Chlamydia-induced foam cell formation utilizes both MyD88-dependent signaling and Trif-dependent IRF3 signaling (33), while zymosan only signals through MyD88. A previous study observed foam cell formation from Pam3CSK4 alone (5). However, this study used peritoneal macrophages elicited with peptone, which could be contaminated with LPS. It is also possible elicitation provides one of the signals necessary for foam cell formation. Likewise, spontaneous foam cell formation in cell lines (23) or primary human macrophages is likely due to cell-type differences. Mice are less susceptible to atherosclerosis than humans, so for in vitro studies murine macrophages may be a more suitable model system. In the BMDM used here, we find that additional stimulation is needed beyond TLR2 ligation, and an exogenous lipid source is necessary. We provide one possible mechanistic link between infection and atherosclerosis.

In addition to Chlamydia, other pathogens can induce foam cell formation. There is a link established between periodontal disease and atherosclerosis (34–36). Periodontopathic bacteria have been isolated from atherosclerotic plaques (37). Similar to Chlamydia infection, TLR2 and TLR4 signaling occurs in the endothelium in response to infection with these bacteria (38). Foam cell formation has also been observed in the context of tuberculosis granuloma formation (10). Based on the results here, we predict that blocking

either Type I IFN production or NF- κ B signaling will reduce the ability of these bacteria to accelerate atherosclerosis.

These data also demonstrate that multiple sources of lipid can drive foam cell formation. We show that in addition to cholesterol carried on LDL or oxLDL particles, chemically defined liposomes can promote foam cell formation. This suggests that circulating MP could promote foam cell formation if NF- κ B activation and Type I IFNs are also present. We show that two types of MP, SRV and ectosomes, have the capacity to induce foam cell formation, including in vivo in a human skin model. There is a growing appreciation for the number of cell types in the body that emit SRV and the biological role these MP play. The concentration of MP circulating in the serum of acute myeloid leukemia patients reaches 75 μ g/mL (39). Here, we found 25 μ g/mL of MV sufficient to promote robust foam cell formation. If circulating MP contained a similar amount of cholesterol to the MV described here, the amount of cholesterol would be 3-fold less than the 50chol liposomes. Hence, we believe 50chol liposomes serve as a simple model system for studying microparticle-induced foam cell formation at physiologically relevant concentrations. We find that a wide variety of MP can induce foam cell formation, and therefore could be directly relevant to atherosclerosis.

Our results expand work performed with platelet and endothelial cell MP to include SRV derived from a range of cell lines and ectosomes. Ectosomes are shed in response to cellular attack by pore-forming toxins (17, 40). Since bacteria produce many pore-forming toxins, we suggest that these ectosomes could provide the source of lipid for foam cell formation in the context of bacterial infections. In the absence of pore-forming toxin, clearance of the bacteria through complement can induce ectosomes (40). Finally, certain strains of oral pathogens themselves secrete MP, which may incorporate TLR ligands (41, 42). Depending on the bacteria and immune response involved, all three components needed for foam cell formation may be present during infection. This model provides a mechanistic link between the invading bacteria and foam cell formation, which can lead to atherosclerosis.

Typically foam cells have an inflammatory phenotype, and oxLDL induces inflammatory cytokines (6). However, the MP and liposomes described here did not induce inflammation on their own. Indeed, the MP blocked TNF α secretion and T cell activation, consistent with an immunosuppressive phenotype. An immunosuppressive phenotype is consistent with the phenotype of MP. SRV released by tumor cells are capable of diminishing cellular responses to IL-2 (43), induce apoptosis in T cells (44, 45) and reduce NK cell lytic capacity (46, 47). Furthermore, they can also express antigens that sequester anti-tumor antibodies, protecting the tumor cell from antibody-dependent cell-mediated cytotoxicity (48). Likewise, MV shed by platelets can be immunosuppressive due to phosphatidylserine and protein expression (49). Importantly, platelet-derived MV inhibit induction of TNF α in macrophages (50), similar to what we observe. Platelet-derived MV are not provoked by toxin attack, but instead are spontaneously shed after 5 days of platelet storage (50). Despite the absence of toxin, these MV are immunosuppressive (50). This suggests that SLO itself does not effect the overall immunosuppressive nature of plasma-membrane derived vesicles. Given that platelet-derived MP account for 70%–90% of circulating MP in blood (51–53), tolerance to these MP may be more important for survival than mounting an inflammatory response to toxin-induced MV. Although these MP impair inflammatory cytokine responses following TLR ligation, they also induce foam cell formation under these circumstances. This widens the range of potentially atherogenic stimuli and reveals novel mechanisms for foam cell formation.

Supplementary Material

Refer to Web version on PubMed Central for supplementary material.

Acknowledgments

We thank members of the Salter lab for helpful discussion and critical reading of the manuscript. We thank Michael Ye for technical assistance. We thank Linton Traub, Meir Aridor and Kimberley Long for advice on liposome preparation, and Simon Watkins at the Center for Biologic Imaging for use of microscopy facilities. We thank Lisa Borghesi and Timothy Billiar for generous gifts of mouse bone marrow.

Abbreviations used

0chol	liposomes containing 0% cholesterol
50chol	liposomes containing 50% cholesterol
BMDM	bone-marrow derived macrophage
MV	ectosomes
MP	microparticles
oxLDL	oxidized LDL
Pam3CSK4	N-palmitoyl-S-[2,3-bis(palmitoyloxy)-(2RS)-propyl]-[R]-cysteiny-[S]-seryl-[S]-lysyl-[S]-lysyl-[S]-lysyl-[S]-lysine
polyI:C	polyinosinic:polycytodilic acid
SRV	spontaneously released microparticles

References

1. Woollard KJ, Geissmann F. Monocytes in atherosclerosis: subsets and functions. *Nat Rev Cardiol.* 2010; 7:77–86. [PubMed: 20065951]
2. Kruth HS. Receptor-independent fluid-phase pinocytosis mechanisms for induction of foam cell formation with native low-density lipoprotein particles. *Curr Opin Lipidol.* 2011; 22:386–393. [PubMed: 21881499]
3. Ye Q, Chen Y, Lei H, Liu Q, Moorhead JF, Varghese Z, Ruan XZ. Inflammatory stress increases unmodified LDL uptake via LDL receptor: an alternative pathway for macrophage foam-cell formation. *Inflamm Res.* 2009; 58:809–818. [PubMed: 19533020]
4. O'Neill LA, Bowie AG. The family of five: TIR-domain-containing adaptors in Toll-like receptor signalling. *Nat Rev Immunol.* 2007; 7:353–364. [PubMed: 17457343]
5. Cao F, Castrillo A, Tontonoz P, Re F, Byrne GI. Chlamydia pneumoniae--induced macrophage foam cell formation is mediated by Toll-like receptor 2. *Infect Immun.* 2007; 75:753–759. [PubMed: 17145941]
6. Stewart CR, Stuart LM, Wilkinson K, van Gils JM, Deng J, Halle A, Rayner KJ, Boyer L, Zhong R, Frazier WA, Lacy-Hulbert A, El Khoury J, Golenbock DT, Moore KJ. CD36 ligands promote sterile inflammation through assembly of a Toll-like receptor 4 and 6 heterodimer. *Nat Immunol.* 2010; 11:155–161. [PubMed: 20037584]
7. Schackelford RE, Misra UK, Florine-Casteel K, Thai SF, Pizzo SV, Adams DO. Oxidized low density lipoprotein suppresses activation of NF kappa B in macrophages via a pertussis toxin-sensitive signaling mechanism. *J Biol Chem.* 1995; 270:3475–3478. [PubMed: 7876078]
8. Heermeier K, Leicht W, Palmethofer A, Ullrich M, Wanner C, Galle J. Oxidized LDL suppresses NF-kappaB and overcomes protection from apoptosis in activated endothelial cells. *J Am Soc Nephrol.* 2001; 12:456–463. [PubMed: 11181793]
9. D'Avila H, Maya-Monteiro CM, Bozza PT. Lipid bodies in innate immune response to bacterial and parasite infections. *Int Immunopharmacol.* 2008; 8:1308–1315. [PubMed: 18687292]

10. Russell DG, Cardona PJ, Kim MJ, Allain S, Altare F. Foamy macrophages and the progression of the human tuberculosis granuloma. *Nat Immunol.* 2009; 10:943–948. [PubMed: 19692995]
11. Zakharova L, Svetlova M, Fomina AF. T cell exosomes induce cholesterol accumulation in human monocytes via phosphatidylserine receptor. *J Cell Physiol.* 2007; 212:174–181. [PubMed: 17299798]
12. Shantsila E, Kamphuisen PW, Lip GY. Circulating microparticles in cardiovascular disease: implications for atherogenesis and atherothrombosis. *J Thromb Haemost.* 2010; 8:2358–2368. [PubMed: 20695980]
13. Chironi G, Simon A, Hugel B, Del Pino M, Garipey J, Freyssinet JM, Tedgui A. Circulating leukocyte-derived microparticles predict subclinical atherosclerosis burden in asymptomatic subjects. *Arterioscler Thromb Vasc Biol.* 2006; 26:2775–2780. [PubMed: 17038634]
14. Leroyer AS, Rautou PE, Silvestre JS, Castier Y, Leseche G, Devue C, Duriez M, Brandes RP, Lutgens E, Tedgui A, Boulanger CM. CD40 ligand+ microparticles from human atherosclerotic plaques stimulate endothelial proliferation and angiogenesis a potential mechanism for intraplaque neovascularization. *J Am Coll Cardiol.* 2008; 52:1302–1311. [PubMed: 18929241]
15. Brown GT, McIntyre TM. Lipopolysaccharide signaling without a nucleus: kinase cascades stimulate platelet shedding of proinflammatory IL-1beta-rich microparticles. *J Immunol.* 2011; 186:5489–5496. [PubMed: 21430222]
16. Boing AN, Hau CM, Sturk A, Nieuwland R. Platelet microparticles contain active caspase 3. *Platelets.* 2008; 19:96–103. [PubMed: 18297548]
17. Keyel PA, Loultcheva L, Roth R, Salter RD, Watkins SC, Yokoyama WM, Heuser JE. Streptolysin O clearance through sequestration into blebs that bud passively from the plasma membrane. *J Cell Sci.* 2011; 124:2414–2423. [PubMed: 21693578]
18. Chu J, Thomas LM, Watkins SC, Franchi L, Nunez G, Salter RD. Cholesterol-dependent cytolytins induce rapid release of mature IL-1beta from murine macrophages in a NLRP3 inflammasome and cathepsin B-dependent manner. *J Leukoc Biol.* 2009; 86:1227–1238. [PubMed: 19675207]
19. Bielli A, Haney CJ, Gabreski G, Watkins SC, Bannykh SI, Aridor M. Regulation of Sar1 NH2 terminus by GTP binding and hydrolysis promotes membrane deformation to control COPII vesicle fission. *J Cell Biol.* 2005; 171:919–924. [PubMed: 16344311]
20. Naiki Y, Sorrentino R, Wong MH, Michelsen KS, Shimada K, Chen S, Yilmaz A, Slepkin A, Schroder NW, Crother TR, Bulut Y, Doherty TM, Bradley M, Shaposhnik Z, Peterson EM, Tontonoz P, Shah PK, Ardit M. TLR/MyD88 and liver X receptor alpha signaling pathways reciprocally control Chlamydia pneumoniae-induced acceleration of atherosclerosis. *J Immunol.* 2008; 181:7176–7185. [PubMed: 18981139]
21. Larregina AT, Morelli AE, Spencer LA, Logar AJ, Watkins SC, Thomson AW, Falo LD Jr. Dermal-resident CD14+ cells differentiate into Langerhans cells. *Nat Immunol.* 2001; 2:1151–1158. [PubMed: 11702065]
22. Kropp LE, Garg M, Binder RJ. Ovalbumin-derived precursor peptides are transferred sequentially from gp96 and calreticulin to MHC class I in the endoplasmic reticulum. *J Immunol.* 2010; 184:5619–5627. [PubMed: 20410492]
23. Funk JL, Feingold KR, Moser AH, Grunfeld C. Lipopolysaccharide stimulation of RAW 264.7 macrophages induces lipid accumulation and foam cell formation. *Atherosclerosis.* 1993; 98:67–82. [PubMed: 8457252]
24. Castrillo A, Joseph SB, Vaidya SA, Haberland M, Fogelman AM, Cheng G, Tontonoz P. Crosstalk between LXR and toll-like receptor signaling mediates bacterial and viral antagonism of cholesterol metabolism. *Mol Cell.* 2003; 12:805–816. [PubMed: 14580333]
25. Zhang L, Chawla A. Role of PPARgamma in macrophage biology and atherosclerosis. *Trends Endocrinol Metab.* 2004; 15:500–505. [PubMed: 15541649]
26. Anderson HC, Mulhall D, Garimella R. Role of extracellular membrane vesicles in the pathogenesis of various diseases, including cancer, renal diseases, atherosclerosis, and arthritis. *Lab Invest.* 2010; 90:1549–1557. [PubMed: 20805791]

27. Eken C, Gasser O, Zenhausern G, Oehri I, Hess C, Schifferli JA. Polymorphonuclear neutrophil-derived ectosomes interfere with the maturation of monocyte-derived dendritic cells. *J Immunol.* 2008; 180:817–824. [PubMed: 18178820]
28. Stein JM, Luzio JP. Membrane sorting during vesicle shedding from neutrophils during sublytic complement attack. *Biochem Soc Trans.* 1989; 17:1082–1083. [PubMed: 2628093]
29. Gasser O, Schifferli JA. Microparticles released by human neutrophils adhere to erythrocytes in the presence of complement. *Exp Cell Res.* 2005; 307:381–387. [PubMed: 15950620]
30. Keyel PA, Heid ME, Salter RD. Macrophage responses to bacterial toxins: a balance between activation and suppression. *Immunol Res.* 2011; 50:118–123. [PubMed: 21717083]
31. Thomas LM, Salter RD. Activation of macrophages by P2X7-induced microvesicles from myeloid cells is mediated by phospholipids and is partially dependent on TLR4. *J Immunol.* 2010; 185:3740–3749. [PubMed: 20709956]
32. D'Avila H, Melo RC, Parreira GG, Werneck-Barroso E, Castro-Faria-Neto HC, Bozza PT. *Mycobacterium bovis* bacillus Calmette-Guerin induces TLR2-mediated formation of lipid bodies: intracellular domains for eicosanoid synthesis in vivo. *J Immunol.* 2006; 176:3087–3097. [PubMed: 16493068]
33. Chen S, Sorrentino R, Shimada K, Bulut Y, Doherty TM, Crother TR, Arditi M. Chlamydia pneumoniae-induced foam cell formation requires MyD88-dependent and -independent signaling and is reciprocally modulated by liver X receptor activation. *J Immunol.* 2008; 181:7186–7193. [PubMed: 18981140]
34. Cotti E, Dessi C, Piras A, Flore G, Deidda M, Madeddu C, Zedda A, Longu G, Mercurio G. Association of endodontic infection with detection of an initial lesion to the cardiovascular system. *J Endod.* 2011; 37:1624–1629. [PubMed: 22099894]
35. Mattila KJ, Nieminen MS, Valtonen VV, Rasi VP, Kesaniemi YA, Syrjala SL, Jungell PS, Isoluoma M, Hietaniemi K, Jokinen MJ. Association between dental health and acute myocardial infarction. *BMJ.* 1989; 298:779–781. [PubMed: 2496855]
36. Lowe GD. Dental disease, coronary heart disease and stroke, and inflammatory markers: what are the associations, and what do they mean? *Circulation.* 2004; 109:1076–1078. [PubMed: 15007017]
37. Toyofuku T, Inoue Y, Kurihara N, Kudo T, Jibiki M, Sugano N, Umeda M, Izumi Y. Differential detection rate of periodontopathic bacteria in atherosclerosis. *Surg Today.* 2011; 41:1395–1400. [PubMed: 21922363]
38. Teles R, Wang CY. Mechanisms involved in the association between periodontal diseases and cardiovascular disease. *Oral Dis.* 2011; 17:450–461. [PubMed: 21223455]
39. Szczepanski MJ, Szajnik M, Welsh A, Whiteside TL, Boyiadzis M. Blast-derived microvesicles in sera from patients with acute myeloid leukemia suppress natural killer cell function via membrane-associated transforming growth factor-beta1. *Haematologica.* 2011; 96:1302–1309. [PubMed: 21606166]
40. Scolding NJ, Morgan BP, Houston WA, Linington C, Campbell AK, Compston DA. Vesicular removal by oligodendrocytes of membrane attack complexes formed by activated complement. *Nature.* 1989; 339:620–622. [PubMed: 2733792]
41. Parent R, Mouton C, Lamonde L, Bouchard D. Human and animal serotypes of *Bacteroides gingivalis* defined by crossed immunoelectrophoresis. *Infect Immun.* 1986; 51:909–918. [PubMed: 3949386]
42. Work E, Knox KW, Vesik M. The chemistry and electron microscopy of an extracellular lipopolysaccharide from *Escherichia coli*. *Ann N Y Acad Sci.* 1966; 133:438–449. [PubMed: 5336349]
43. Clayton A, Mitchell JP, Court J, Mason MD, Tabi Z. Human tumor-derived exosomes selectively impair lymphocyte responses to interleukin-2. *Cancer Res.* 2007; 67:7458–7466. [PubMed: 17671216]
44. Kim JW, Wieckowski E, Taylor DD, Reichert TE, Watkins S, Whiteside TL. Fas ligand-positive membranous vesicles isolated from sera of patients with oral cancer induce apoptosis of activated T lymphocytes. *Clin Cancer Res.* 2005; 11:1010–1020. [PubMed: 15709166]

45. Taylor DD, Gercel-Taylor C, Lyons KS, Stanson J, Whiteside TL. T-cell apoptosis and suppression of T-cell receptor/CD3-zeta by Fas ligand-containing membrane vesicles shed from ovarian tumors. *Clin Cancer Res.* 2003; 9:5113–5119. [PubMed: 14613988]
46. Liu C, Yu S, Zinn K, Wang J, Zhang L, Jia Y, Kappes JC, Barnes S, Kimberly RP, Grizzle WE, Zhang HG. Murine mammary carcinoma exosomes promote tumor growth by suppression of NK cell function. *J Immunol.* 2006; 176:1375–1385. [PubMed: 16424164]
47. Clayton A, Mitchell JP, Court J, Linnane S, Mason MD, Tabi Z. Human tumor-derived exosomes down-modulate NKG2D expression. *J Immunol.* 2008; 180:7249–7258. [PubMed: 18490724]
48. Battke C, Ruiss R, Welsch U, Wimberger P, Lang S, Jochum S, Zeidler R. Tumour exosomes inhibit binding of tumour-reactive antibodies to tumour cells and reduce ADCC. *Cancer Immunol Immunother.* 2011; 60:639–648. [PubMed: 21293856]
49. Sadallah S, Eken C, Schifferli JA. Ectosomes as modulators of inflammation and immunity. *Clin Exp Immunol.* 2011; 163:26–32. [PubMed: 21039423]
50. Sadallah S, Eken C, Martin PJ, Schifferli JA. Microparticles (ectosomes) shed by stored human platelets downregulate macrophages and modify the development of dendritic cells. *J Immunol.* 2011; 186:6543–6552. [PubMed: 21525379]
51. Horstman LL, Ahn YS. Platelet microparticles: a wide-angle perspective. *Crit Rev Oncol Hematol.* 1999; 30:111–142. [PubMed: 10439058]
52. Berckmans RJ, Nieuwland R, Boing AN, Romijn FP, Hack CE, Sturk A. Cell-derived microparticles circulate in healthy humans and support low grade thrombin generation. *Thromb Haemost.* 2001; 85:639–646. [PubMed: 11341498]
53. Joop K, Berckmans RJ, Nieuwland R, Berkhout J, Romijn FP, Hack CE, Sturk A. Microparticles from patients with multiple organ dysfunction syndrome and sepsis support coagulation through multiple mechanisms. *Thromb Haemost.* 2001; 85:810–820. [PubMed: 11372673]

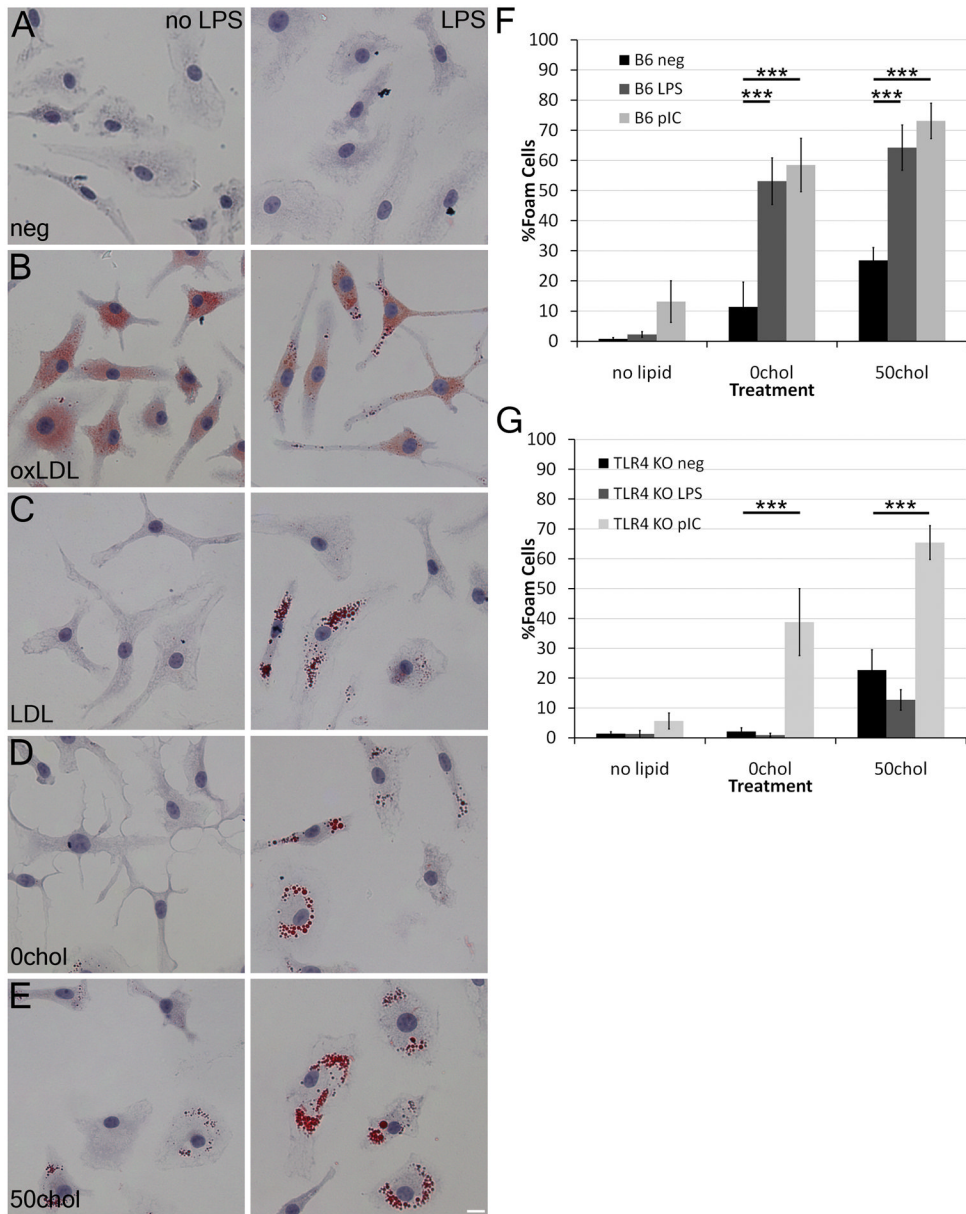


Figure 1. LPS combined with lipids promote foam cell formation in macrophages
 (A-E) BMDM were cultured with the indicated lipids in the presence or absence of 10 ng/mL LPS for 2 days at 37°C, fixed and stained with Oil Red O and hematoxylin. (F-G) BMDM from B6 (F) or TLR4^{-/-} (G) mice were cultured with LPS or 10 μg/mL poly I:C in the presence of the indicated lipid sources. The number of foam cells was quantitated. Mean ± SEM are shown. An average of 580 cells from 3–9 independent experiments were counted for each condition. *** indicate p<0.001 from liposomes only. Scale bar = 10 μm.

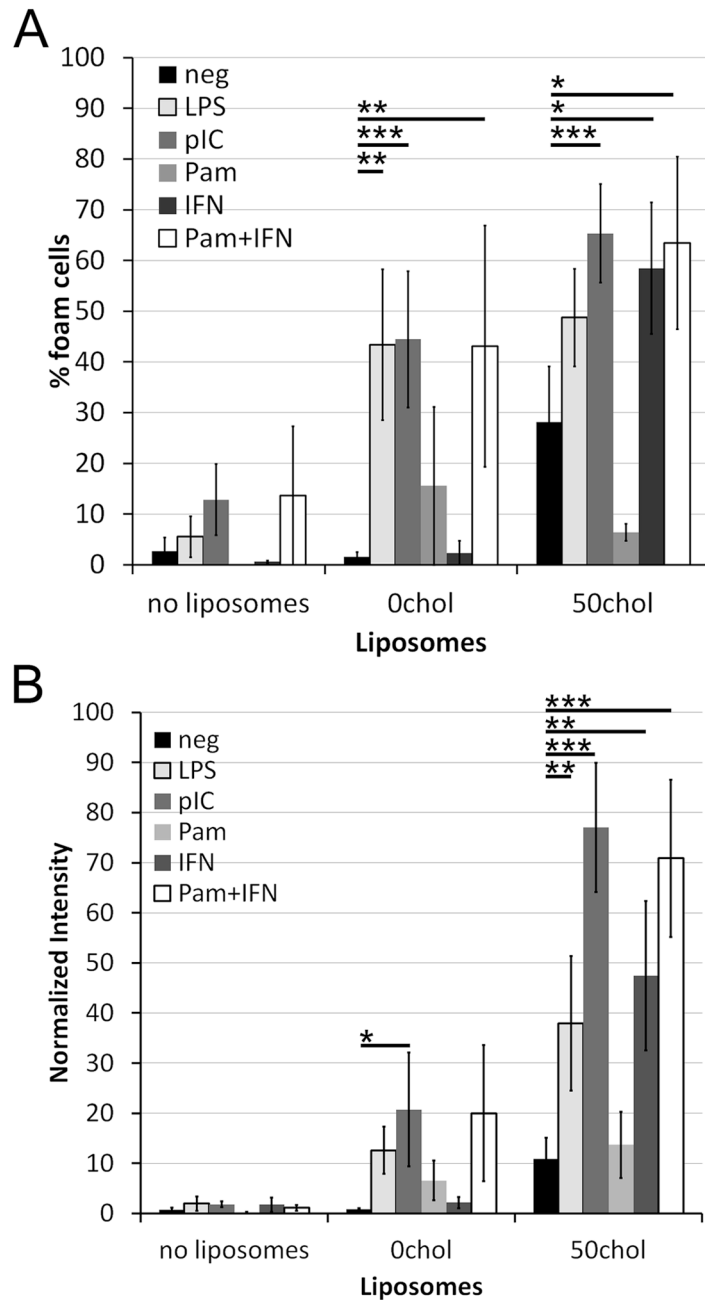


Figure 2. Synergism between TLR and type I IFN signaling for foam cell formation
 BMDM from B6 mice were treated as described in Fig 1. Pam3CSK4 (Pam) or IFN α were included at 1 μ g/mL or 100 U/mL, respectively, where indicated. (A) The number of foam cells were counted, or (B) the intensity of Oil Red O staining was measured and normalized using Metamorph. An average of 650 cells from 3–7 independent experiments were counted for each condition. * indicates $p < 0.05$, ** $p < 0.01$, *** $p < 0.001$ from liposomes only.

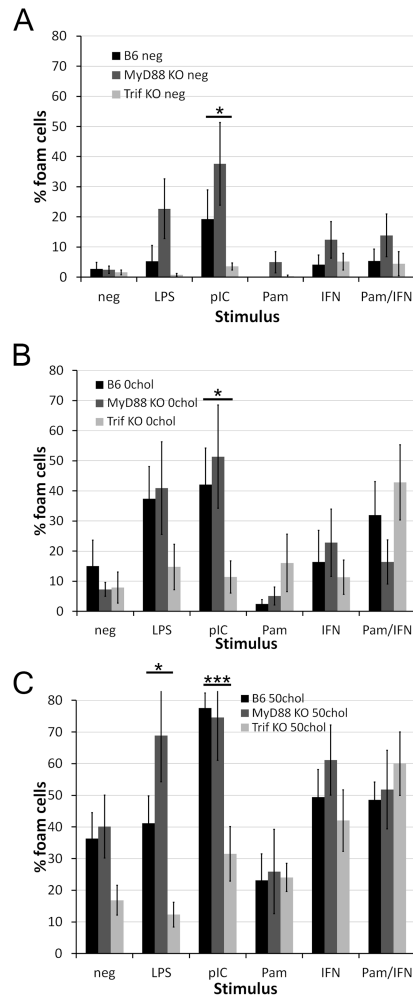


Figure 3. Trif is required for foam cell formation

BMDM from B6, MyD88^{-/-} or Trif^{-/-} mice were treated and quantitated as described in Fig 1 with no lipid source (A) or liposomes composed of either 0% (B) or 50% (C) cholesterol. An average of 1300 cells from 9 independent experiments were counted for B6 and Trif^{-/-} and an average of 1000 cells from 6 independent experiments were counted for MyD88^{-/-}. * indicates p<0.05, *** p<0.001 from B6.

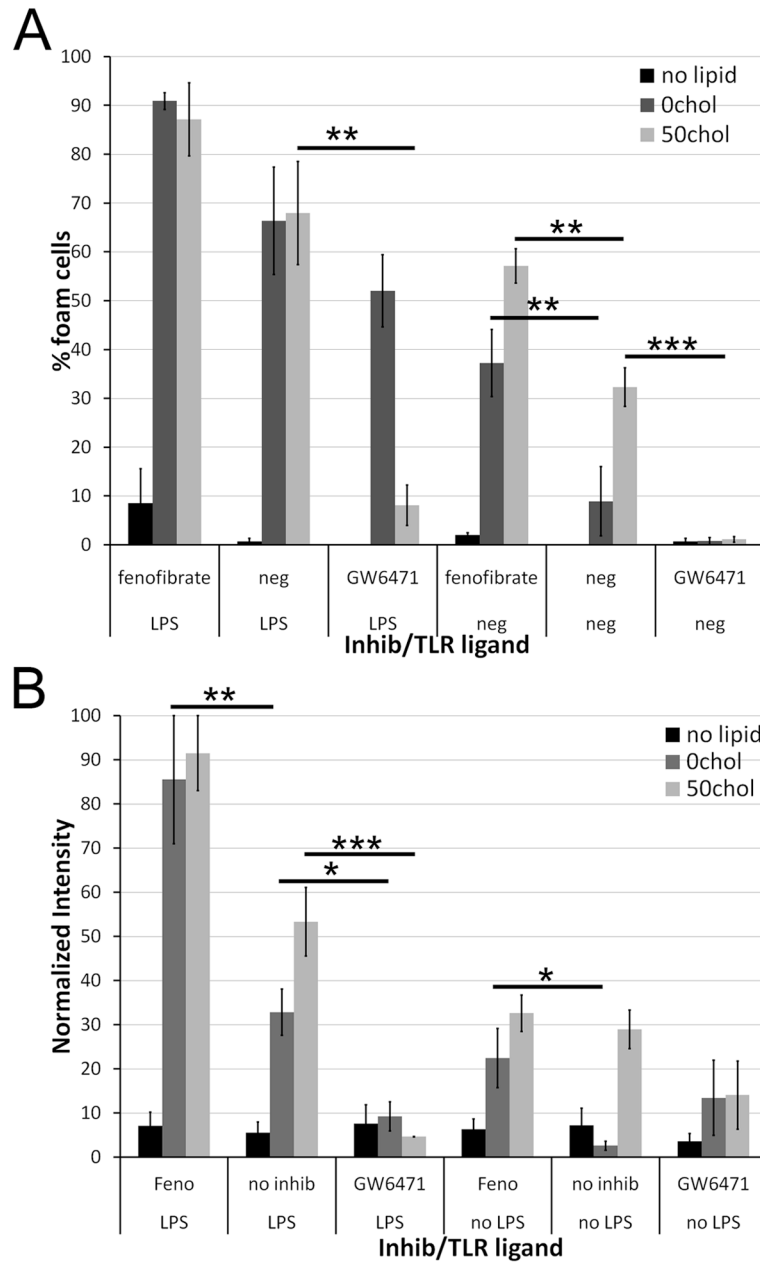


Figure 4. PPAR α is needed for foam cell formation

BMDM were treated as described in Fig 1, except that PPAR α agonist fenofibrate or PPAR α antagonist GW6471 were included where indicated. (A) The number of foam cells or (B) the intensity of Oil Red O staining was quantitated. An average of 500 cells from 5 independent experiments was counted for each condition. * $p < 0.05$, ** $p < 0.01$, *** $p < 0.001$ compared to no inhibitors.

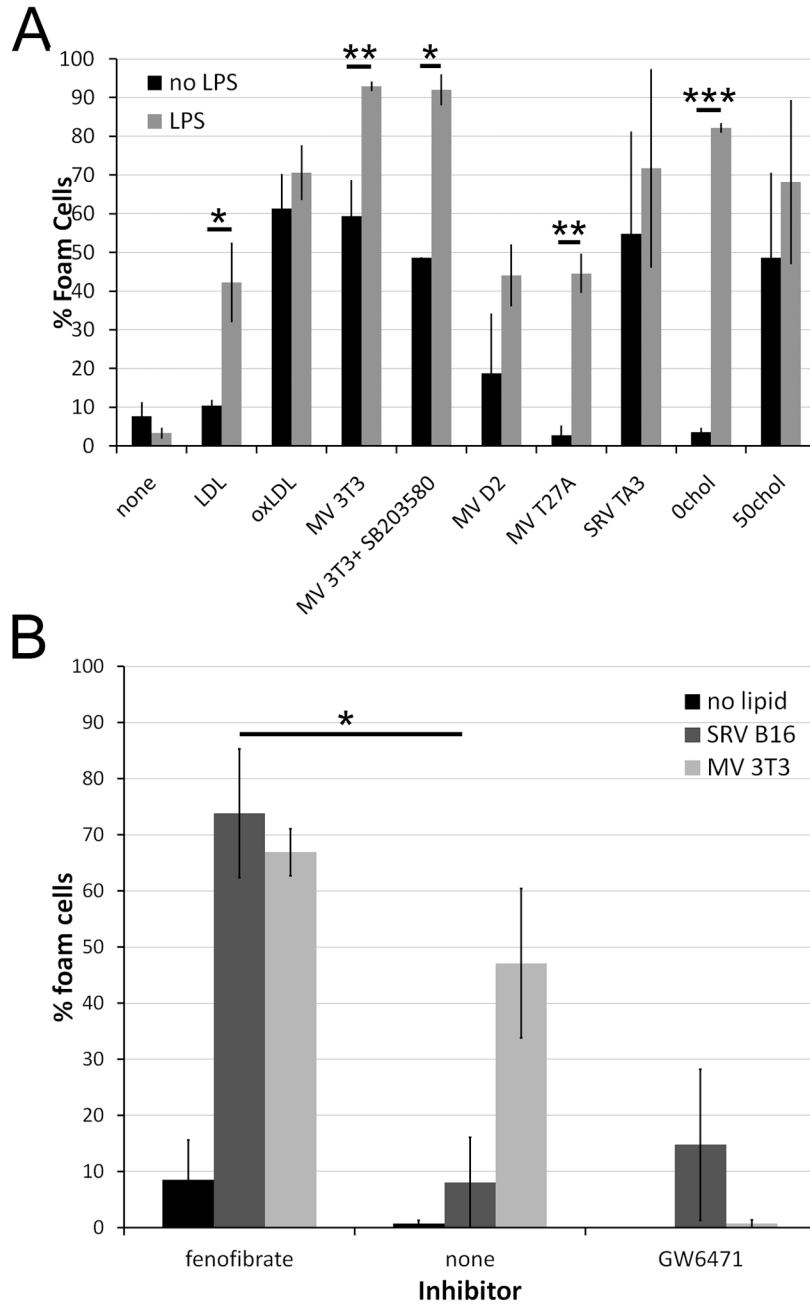


Figure 5. Microparticles promote foam cell formation

Microvesicles were generated by treating the indicated cell lines with sublytic doses of SLO for 15 minutes at 37°C (MV) or collecting spontaneously released particles from cultures (SRV) and centrifuging the supernatants at 107,000xg. The pellet was resuspended and added to BMDM in the presence or absence of 10 ng/mL LPS as cells treated as in Fig 1. Approximate cholesterol levels in MV were 2.5 $\mu\text{g/mL}$ (3T3), 1.2 $\mu\text{g/mL}$ (D2) and 0.6 $\mu\text{g/mL}$ (T27A). In addition to microparticles, BMDM received either LPS (A) or LPS plus PPAR α agonist and antagonist (B). For each condition, an average of 700 cells from 3–9 independent experiments (A) or 350 cells from 3 experiments (B) were counted. * $p < 0.05$, ** $p < 0.01$ or *** $p < 0.001$ compared to no LPS (A) or no inhibitor (B).

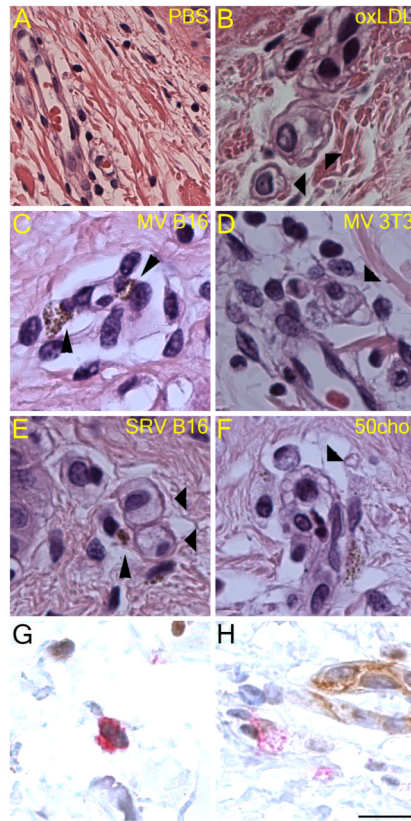


Figure 6. Microparticles promote foam cell formation in a human skin model

Microparticles from the indicated sources or 50chol liposomes were injected intradermally into skin explants, cultured for 3 days at 37°C fixed in formaldehyde, embedded in paraffin, sectioned and stained with hematoxylin and eosin (A-F) or stained with anti-CD68 (red) and anti-CD31 (brown) to identify macrophages and endothelial cells, respectively (G-H). Images illustrate clearly the presence of macrophages with clear and vacuolated cytoplasm characteristic of foam cells, shown by thick arrowheads. Thin arrowheads indicate microparticles derived from B16 cells, which contain melanin. Images from one representative experiment of two performed is shown. Scale bar = 20 μm .

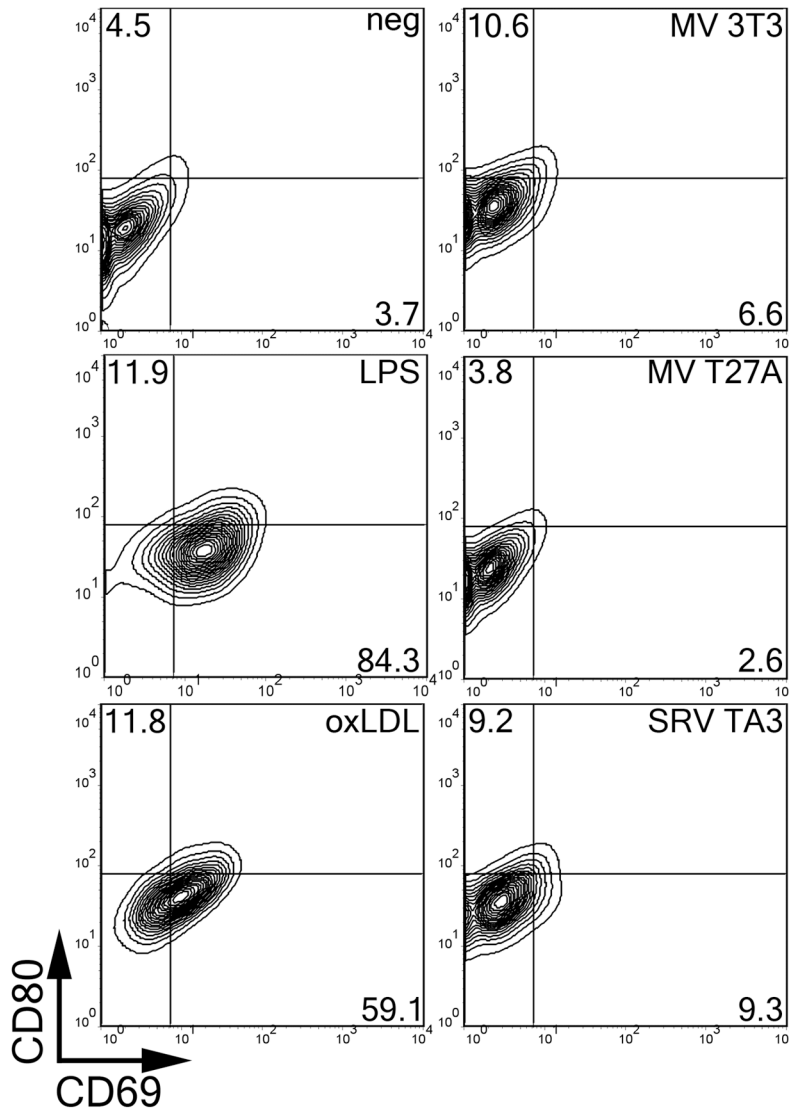


Figure 7. Microparticles promote weak activation of macrophages

BMDM were treated with the indicated lipid source or LPS for 18 hours at 37°C, harvested, stained with anti-CD80 conjugated to APC and anti-CD69 conjugated to FITC and analyzed by FACS. Percentages of cells expressing high levels of CD80 or CD69 are shown. Representative FACS plots are shown from 16 independent experiments.

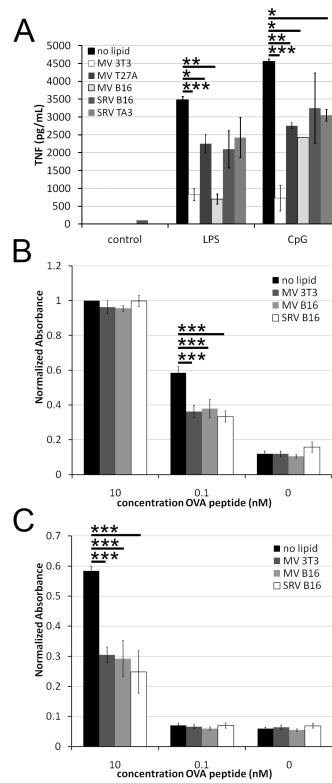


Figure 8. Microparticles are immunosuppressive

(A) TNF α levels in supernatants from BMDM treated as in Fig 7, or with the addition of 10 ng/mL LPS or 1.68 μ M CPG were measured by ELISA. (B-C) B3Z cells in the presence (B) or absence (C) of B16 cells were pulsed with the indicated concentration of OVA peptide and the indicated microparticles for 18 hours at 37°C, and analyzed for β -galactosidase production. Absorbance values were normalized to 1 for B3Z cells treated with 10 nM OVA peptide. P values are compared to no lipid and are * p <0.05, ** p <0.01, *** p <0.001.